ISSN 1990-7931, Russian Journal of Physical Chemistry B, 2017, Vol. 11, No. 4, pp. 624–634. © Pleiades Publishing, Ltd., 2017.
Original Russian Text © I.V. Kumpanenko, A.V. Roshchin, N.A. Ivanova, A.V. Bloshenko, T.S. Volchenko, 2017, published in Khimicheskaya Fizika, 2017, Vol. 36, No. 8, pp. 3–13.

CHEMICAL PHYSICS OF ECOLOGICAL PROCESSES

Calculation of Space–Time Concentration Profiles of Contaminants in a Fixed Sorbent Bed from Experimental Data on Dynamic Water Purification

I. V. Kumpanenko*, A. V. Roshchin, N. A. Ivanova, A. V. Bloshenko, and T. S. Volchenko

Semenov Institute of Chemical Physics, Russian Academy of Sciences, Moscow, 119991 Russia

**e-mail: ivkumpan@chph.ras.ru*

Received December 9, 2016

Abstract—A formula for a mathematical description of the relationship between the breakthrough curve $C(t)/C_0$ for the dynamic sorption purification of water and the space–time concentration profile of contaminant $q(x, t)$ in the fixed sorbent bed is derived. The derivation is based on the simplifying assumption that the dependence of the adsorbate concentration profile $q(x, t)$ on the longitudinal coordinate x of the bed is described by the logistic function $q(x, t) = a/\{1 + \exp\{-k(t)[x - b(t)]\}\}$, in which a is a constant and the time-dependent parameters $k(t)$ and $b(t)$ are expanded into the power series $k(t) = k_0 + k_1t + k_2t^2$ and $b(t) = b_0 + b_1t + b_2t^2 + b_3t^3 + b_4t^4$ with the expansion coefficients b_0, b_1, b_2, b_3, b_4, k_0, k_1, and k_2, so that $C(t)/C_0 = 1 - (S/(C_0v))F(t, b_0, b_1, b_2, b_3, b_4, k_0, k_1, k_2)$, where $C(t)$ is the breakthrough concentration of contaminant in the water effluent from at the fixed bed, C_0 is the concentration of the contaminant in the water influent into the fixed bed, S is the cross-sectional area of the bed, v is the water flow rate, and F is a definite analytic function dependent on the profile $q(x, t)$. The coefficients b_0, b_1, b_2, b_3, b_4, k_0, k_1, and k_2 are determined by fitting the theoretical breakthrough curve to the experimental one. With the help of this approach, space–time profiles for dynamic water purification from lead, nitrate, and perchlorate ions are calculated. It is shown that the adsorbed contaminant ions are redistributed between different parts of the fixed bed in the course of the adsorption process.

Keywords: fixed sorbent bed, space–time concentration profile, contaminants, effluent curve, breakthrough concentration, redistribution of ions

DOI: 10.1134/S1990793117040194

1. INTRODUCTION

Recent years has seen an upsurge of interest in studying the process of adsorbate accumulation in the fixed sorbent bed during the purification of aqueous media from contaminants in the dynamic mode [1–6]. One of the directions of research in this area is the analysis of the adsorbate concentration distribution along the axis of the sorption bed and its relationship to the time dependence of the breakthrough concentration of contaminants in the water effluent from this bed.

In our previous article [7], devoted to the study of space–time profiles of mercury ion concentrations in a fixed ionite bed for the process of sorption water purification, it was shown that the time dependence of the breakthrough concentration of contaminants C (mg/cm^3) at the outlet from the sorption column is given by

$$C(t) = C_0 - \frac{S}{v}\int_0^L \frac{\partial q(x,t)}{\partial t}\,dx, \qquad (1)$$

where C_0 is the concentration of contaminants in the water entering the fixed bed, mg/cm^3; S is the cross-sectional area of the bed, cm^2; L is the height of the bed, cm; v is the volumetric flow rate of water, cm^3/min; $q(x, t)$ is the concentration of contaminants in the fixed sorbent bed at the point of its measurement with coordinate x at time t, mg/cm^3; the function $q(x, t)$ describes the space–time profile of the concentrations of contaminants along the sorbent bed; x is the distance from the inlet of the fixed bed to the point of measurement of the concentration $q(x, t)$, cm; and t is the current time, min.

This formula was used to calculate the breakthrough curve $C(t)$ for the dynamic sorption of mercury on the basis of the data we obtained from experiments on measuring the distribution of the mercury

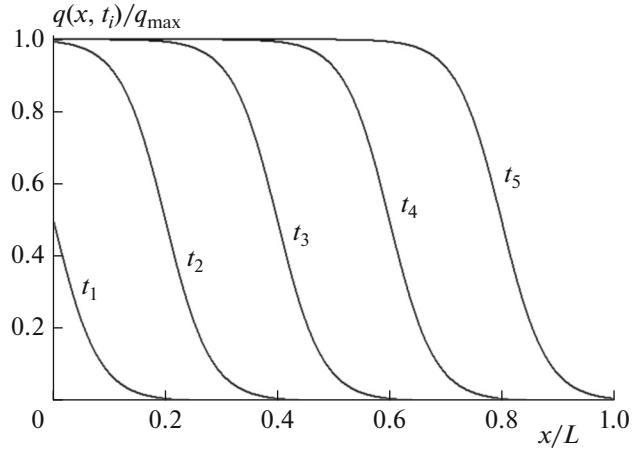

Fig. 1. Schematic plot of the time evolution of the concentration distribution $q(x, t)$ over the height of the fixed sorbent bed. The flow of aqueous solution of contaminant moves from left to right; $t_1 < t_2 < ... < t_5$ are the times of concentration measurements.

concentration along the axis of the fixed bed as a function of the time, $q(x, t)$. The calculated breakthrough curve was compared with a curve determined using traditional methods. A good match between the two curves was observed.

Thus, the paper [7] have demonstrated the possibility of directly calculating the breakthrough curve $C(t)$ from the experimentally determined function $q(x, t)$. In the present paper, in order to develop the theoretical approach described in [7], we describe a method for solving the inverse problem of calculating the space–time profile of the adsorbate concentrations $q(x, t)$ on the basis of experimental data on the breakthrough curve $C(t)$. The method is tested on published experimental data.

2. THEORETICAL FOUNDATIONS OF THE METHOD

Recall that, in the derivation of formula (1), no assumptions were made as to the nature of the adsorbent, the aggregate state of the mobile phase, the origin and structure of the sorbent, the shape and dimensions of the sorption column, the mechanism of the sorption process, etc. The only assumption was that the law of conservation of mass holds; therefore, this formula is of a general nature.

Since the variables x and t are independent, the order of integration–differentiation can be interchanged and formula (1) can be recast as

$$C(t) = C_0 - \frac{S}{v}\frac{\partial\int_0^L q(x,t)dx}{\partial t}.$$

For reasons of convenience, in the scientific literature, the dimensionless ratio of the current breakthrough concentration of contaminant $C(t)$ at the outlet from the sorption column to the initial concentration of contaminant C_0 in water entering the fixed bed, $C(t)/C_0$, is often used to describe the breakthrough curves. This ratio is given by

$$\frac{C(t)}{C_0} = 1 - \frac{S}{C_0 v}\frac{\partial\int_0^L q(x,t)dx}{\partial t}. \quad (2)$$

It is in this form that the functional dependence describing the breakthrough curves is presented in the current article.

Obviously, after calculating the definite integral in formula (2), information on the form of the dependence of the contaminant concentration q in the fixed bed on the x coordinate disappears. Therefore, to solve the above inverse problem, i.e., to calculate the space–time profile $q(x, t)$ using expression (2) and the dependence $C(t)$ only as a function of time t, without introducing any additional assumptions about the behavior of the dependence of q on x is impossible.

In this connection, let us examine the published data on studying the distribution of adsorbate in a fixed sorbent bed. Theoretically, this issue was considered quite often and in detail [8, 9]. However, experimentally, the concentration distribution of adsorbate in the sorption bed has been studied much less frequently [7, 10–13]. Both theoretical and experimental studies show that the dependence of $q(x, t)$ on x is described by a descending sigmoidal curve, the inflection point of which moves with time in the direction of increasing x (Fig. 1).

Figure 1 schematically shows how the concentration of adsorbate in the fixed bed is distributed along the sorption column axis and how this distribution varies with time. The ordinate represents the ratio of the concentration $q(x, t_i)$ at the current measurement point x at time t_i to the maximum concentration of contaminant q_{max} in the sorbent recorded during the experiment. The value of q_{max} correlates with the dynamic adsorption capacity of the sorbent, although, as experiments show, it most often does not reach the value of the latter. The abscissa represents the ratio of the distance from the sorption bed inlet to the measurement point x to the height of the bed L.

In general, such curves are most closely described by the logistic function [7]:

$$y = \frac{a}{1 + \exp\{-k(x - b)\}}. \quad (3)$$

At $k < 0$, this function is descending: at $x \to +\infty$, $y \to 0$ and at $x \to -\infty$, $y \to a$. The parameters k and b characterize, respectively, the "width" of the descend-

ing branch of the curve and the x coordinate of its inflection point.

Note that, according to most experimental studies, the breakthrough curves describing the time dependence of $C(t)/C_0$ also have a logistic form, but only ascending, i.e., expression (3) with $k > 0$. In some works, such a description is called the Yoon–Nelson model [14, 15].

In one of our previous works [16], it was pointed out that, if the dependence of the concentration of adsorbate q in the sorbent bed on the coordinate x is given by logistic function (3), then the dependence of this concentration on the time can be provided by making the parameters a, b, and k in (3) time-dependent. Clearly, it is unlikely that the parameter a, which identical to the aforementioned quantity q_{max}, associated with the dynamic adsorption capacity of the sorbent, can depend on the time. Most likely, the dependence of function (3) is associated with a time dependence of the parameter b, which is "responsible" for the movement of the logistic curves (Fig. 1) with time. Although, given that the "width" of the descending branch of the curves increases with time, it cannot be excluded that the parameter k, responsible for such a broadening, is time-dependent.

Taking into account the foregoing, we assumed that the dependences of the space–time concentration profile of contaminants on the coordinate and time in the fixed sorbent bed can be described by the formula

$$q(x,t) = \frac{a}{1+\exp\{-k(t)[x-b(t)]\}}. \quad (4)$$

Introducing the function $q(x, t)$ in form (4) into (2), we can solve the problem of calculating the space–time concentration profile of adsorbate $q(x, t)$ from measured breakthrough curves $C(t)$.

To do this, we should first integrate $q(x, t)$ over x from 0 to L:

$$\int_0^L q(x,t)dx = \int_0^L \frac{a}{1+\exp\{-k(t)[x-b(t)]\}}dx = \frac{a}{k(t)}\left\{\ln\frac{1+\exp\{k(t)[L-b(t)]\}}{1+\exp\{-k(t)b(t)\}}\right\}. \quad (5)$$

The next step is to differentiate this integral with respect to t:

$$\frac{\partial\int_0^L q(x,t)dx}{\partial t} = a\left\{-\frac{k'(t)}{k^2(t)}\ln\frac{1+\exp\{k(t)[L-b(t)]\}}{1+\exp\{-k(t)b(t)\}} + \frac{1}{k(t)}\left[\frac{\exp\{k(t)[L-b(t)]\}\{k'(t)[L-b(t)]-k(t)b'(t)\}[1+\exp(-k(t)b(t)\}]}{\{1+\exp\{k(t)[L-b(t)]\}\}[1+\exp\{-k(t)b(t)\}]} + \frac{\exp\{-k(t)b(t)\}[k'(t)b(t)+k(t)b'(t)]\{1+\exp\{k(t)[L-b(t)]\}\}}{\{1+\exp\{k(t)[L-b(t)]\}\}[1+\exp\{-k(t)b(t)\}]}\right]\right\}, \quad (6)$$

where $b'(t)$ and $k'(t)$ are the first derivatives of the functions $b(t)$ and $k(t)$ with respect to the time.

The form of the functions $b(t)$ and $k(t)$ is unknown. However, it can be assumed that, within relatively narrow time intervals, they can be described by simple power series expansion with a small number of terms. Our further calculations showed that such an assumption is entirely reasonable.

So, we assumed that

$$b(t) = b_0 + b_1t + b_2t^2 + b_3t^3 + b_4t^4, \quad k(t) = k_0 + k_1t + k_2t^2. \quad (7)$$

Then, the first derivatives of these functions with respect to the time read as

$$b'(t) = \frac{\partial b(t)}{\partial t} = b_1 + 2b_2t + 3b_3t^2 + 4b_4t^3, \quad k'(t) = \frac{\partial k(t)}{\partial t} = k_1 + 2k_2t. \quad (8)$$

Substituting formulas (7) and (8) for the dependences $b(t)$, $k(t)$, $b'(t)$, and $k'(t)$ into expression (6) for the derivative of the integral and introducing the latter into (2), we obtain the final equation for calculating the parameters of the sought space–time profile. Because of the awkwardness of this equation, we do not give it here completely, showing only schematically. To this end, let us denote the derivative of integral (6) with the power series expansion (7) and (8) substituted in it as $F(t, b_0, b_1, b_2, b_3, b_4, k_0, k_1, k_2)$, i.e., as a function of one variable t, dependent also on the variable (in the case under consideration, a limited number of terms of power series expansion, namely eight) parameters $b_0, b_1, \ldots, k_2$.

In this notation, the equation for determining the parameters of the desired space–time profile has the form

$$\frac{C(t)}{C_0} = 1 - \frac{S}{C_0V}F(t, b_0, b_1, b_2, b_3, b_4, k_0, k_1, k_2). \quad (9)$$

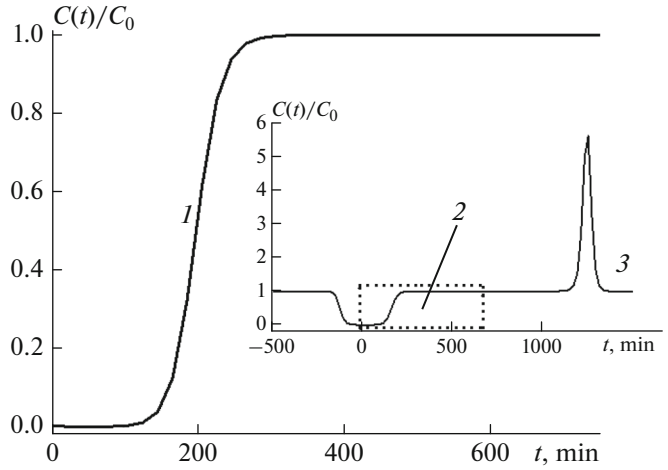

Fig. 2. Breakthrough curve *1* within rectangular region *2* with the time and concentration intervals of $0 < t < 700$ min and $0 < C(t)/C_0 < 1$, respectively, cut out from curve *3*, calculated by Eq. (9) within $-500 < t < 1500$ min.

The constants C_0, S, and v, appearing explicitly in Eq. (9), as well as the constants a and L, implicitly entering through Eq. (6), are introduced in advance, being determined by the experimental conditions. The dependence of $C(t)$ is obtained experimentally. Thus, the variable parameters b_0, b_1, b_2, b_3, b_4, k_0, k_1, and k_2 entering into Eq. (9) can be determined using any known methods for fitting the theoretical dependence $C(t)$ to the experimental one.

Substituting (7) into (4) and assuming for simplicity that $a = 1$, we obtain a simple analytic expression for calculating the space–time concentration profile of contaminants in the fixed sorbent bed:

$$q(x,t) = \frac{1}{1 + \exp\{-(k_0 + k_1 t + k_2 t^2)[x - (b_0 + b_1 t + b_2 t^2 + b_3 t^3 + b_4 t^4)]\}}. \quad (10)$$

Having the set of parameters b_0, b_1, b_2, b_3, b_4, k_0, k_1, and k_2, determined in the aforementioned process, it is easy to calculate the required space–time concentration profile by formula (10).

In the next section, we demonstrate the application of the described method for calculating the space–time profiles from measured breakthrough curves $C(t)$ reported in the literature.

3. APPLICATION OF THE DEVELOPED METHOD

Before proceeding with determining the variable parameters in Eq. (9) by fitting the theoretical to the experimental $C(t)/C_0$ dependence, it is desirable to have an idea of the general form of this dependence within a large time interval and of the effect on it of those or other variable parameters. This information would help establish the initial values of these parameters in the iterative process of fitting.

Figure 2 shows initial curve *3* calculated by Eq. (9) at $a = 1$ within the argument interval $-500 < t < 1500$ min, and the portion of the curve "cut out" from it within $0 < t < 700$ min, which can serve as a starting curve for fitting to the experimental breakthrough curve. The initial curve of function (9) was calculated over the widest range of the argument (time t), formally including its negative values, at arbitrarily chosen values of the variable parameters and constants: $b_0 = 50$, $b_1 = 0.07$, $b_2 = b_3 = b_4 = 0$, $k_0 = -0.6$, $k_1 = 0.0008$, $k_2 = 0$, $L = 20$, $S = 3$, $v = 3$, and $C_0 = 0.07$.

This made it possible to reveal the location of the portion of the curve with a characteristic sigmoidal form. Then, a preliminary "manual" adjustment of these parameters enabled to position the chosen sigmoidal segment of the curve within a reasonable time interval (Fig. 2). Note that, in our case, the choice of the initial values of the variable parameters used in the iterative process of fitting the theoretical function to the experimental values, turned out to be quite a painstaking task.

In the following subsections of this article, we presented the results of a theoretical treatment of the published experimental data on breakthrough curves for the dynamic adsorption of contaminants from aque-

Table 1. Variables, variable parameters, and constants for breakthrough curves and space–time concentration profiles used in the theoretical treatment of experimental data

Contaminant	x, mm	t, min	b_0	b_1	b_2	b_3	b_4	k_0
Pb-activated carbon [14]	0–100	0–2000	18.97	0.0143	1.276×10^{-5}	0	0	–0.287
Nitrates: (NO_3^-) PAN-oxime-nano [17]	0–150	0–2100	27.6	0.04	-3×10^{-6}	0	0	–0.387
Perchlorates: (ClO_4^-)–CLDH [18]	0–85	0–700	9.2994	0.0437	-1.405×10^{-6}	0	0	–2.4

Contaminant	k_1	k_2	C_0, mg/cm^3	L, mm	S, cm^2	v, cm^3/min	a, mg/cm^3	
Pb–activated carbon [14]	8×10^{-4}	0	0.1	100	7	10	1	
Nitrates: (NO_3^-) PAN-oxime-nano [17]	1.76×10^{-4}	0	0.05	150	0.2	2.5	1	
Perchlorates: (ClO_4^-)–CLDH [18]	0.0034	0	0.1	85	0.5	2	1	

ous solutions on various sorbents within the framework of the above-described method. Specifically, the results of studying the adsorption of Pb^{2+} ions on activated carbon [14], nitrate ions on nanofiber polyacrylonitrile modified with amidoxime groups (PAN-oxime-nano) [17], and perchlorate ions on calcined layered double hydroxide (CLDH) Al/Zn [18]. The constants (C_0, L, S, a) used in the calculations are listed in Table 1, wherein the intervals of variation of x and t, as well as the values of the variable parameters obtained from the fitting, are also given.

Dynamic Adsorption of Lead on Activated Carbon

In [14], devoted to studying the process of water purification from heavy metals by means of a column containing a fixed bed of sorbent, the influence of the water flow rate v through the sorbent bed, sorbent bed height L, and initial concentration C_0 of Pb^{2+} and Cu^{2+} ions in water on the form of the breakthrough curves was studied. The sorbent was activated charcoal prepared from the pits of fruits of Palmyra palm tree.

In Fig. 3 the circles represent the experimental breakthrough curve [14] obtained by measuring the concentration of Pb^{2+} ions in the aqueous solution at the outlet of the sorption column at an effluent flow rate of $v = 10$ cm^3/min and an initial concentration of $C_0 = 0.1$ mg/cm^3. The constants describing the geometry of the fixed sorbent bed are $L = 100$ mm and $S = 7$ cm^2.

The experimental dependence shown in Fig. 3 was theoretically approximated by adjusting the parameters b_0, b_1, b_2, b_3, b_4, k_0, k_1, and k_2 according to the Levenberg–Marquardt iterative method, in which the set of experimental points in the two-dimensional space $\{t, C/C_0\}$ was described by theoretical function (9). The quality of fitting of function (9) to the experimental points, estimated from the value of the determination coefficient, which turned out to be $R^2 = 0.999333$, is quite high. The values of the variable parameters

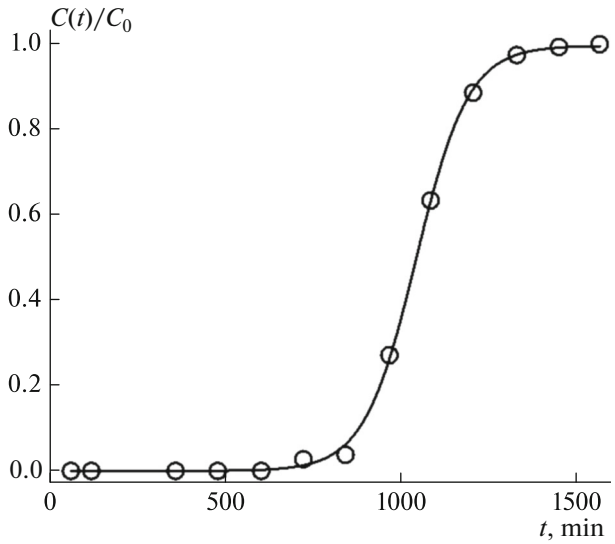

Fig. 3. Time dependence of the concentration ratio $C(t)/C_0$ for Pb^{2+} ions in the aqueous solution at the outlet from the sorption column. The circles represent the experimental data from [14]. The line is the result of fitting theoretical dependence (9) to the experimental one.

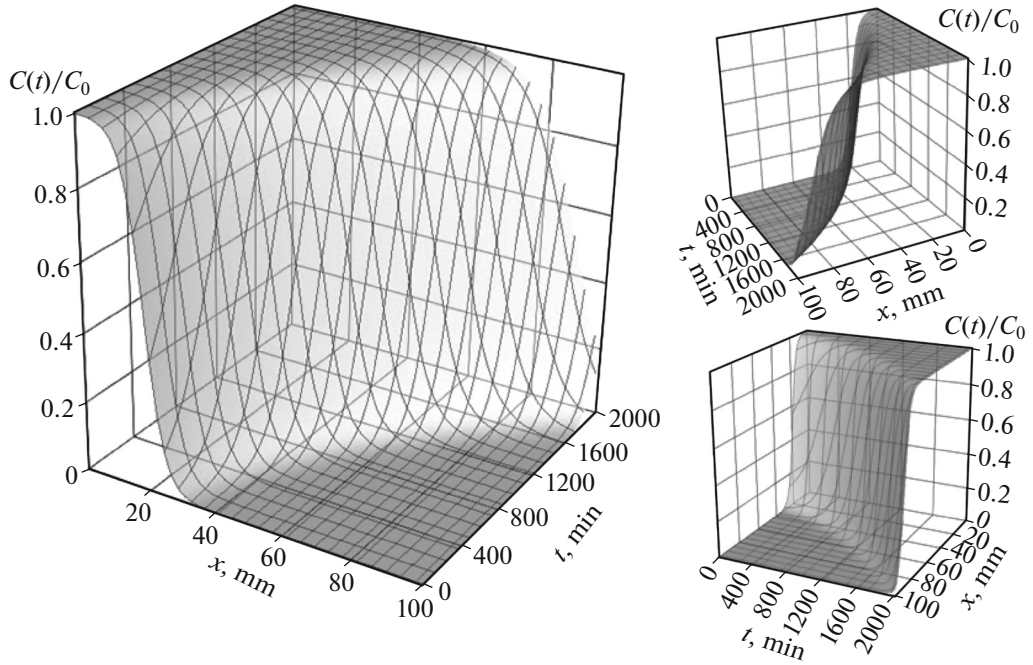

Fig. 4. Space–time concentration profile of Pb^{2+} in a fixed activated carbon bed for water purification from lead.

obtained from the approximation are listed in the table. It turned out that the coefficients b_3, b_4, and k_2 of the higher terms of power series expansion (7) for the expansion of the functions $b(t)$ and $k(t)$ are zeros. In other words, five parameters, b_0, b_1, b_2, k_0, and k_1, are sufficient for a full description of the breakthrough curve, and therefore, the space–time concentration profile.

Using the parameter values presented in the table, a space–time concentration profile of the mercury ion in a fixed activated carbon bed was calculated. A 3D view of the profile is shown in Fig. 4.

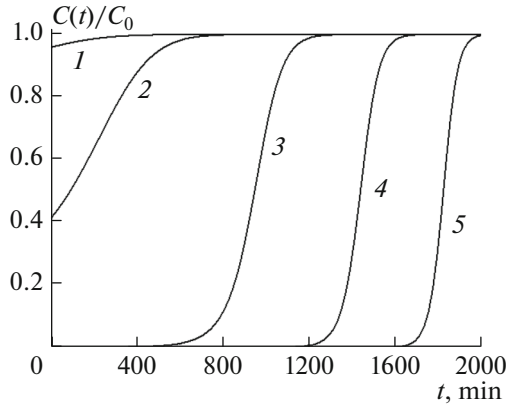

Fig. 5. Time dependence of the concentration ratio $C(t)/C_0$ for lead ions in a fixed activated carbon bed at various points x (mm): (*1*) 10, (*2*) 20, (*3*) 40, (*4*) 60, and (*5*) 80.

For better perception of the shape of the profile, it is shown in three project views. Figure 4 illustrates the general features of the time evolution of the concentration profile of a substance in the fixed sorbent bed: with time, the position of the concentration curve (as defined by the inflection point) moves monotonically from the inlet to the outlet of the bed. It is as a result of this displacement that a breakthrough occurs at the outlet of the sorption column. Another feature of this profile is the monotonic increase in the lead concentration at any point of the fixed bed in time, regardless of its coordinate x. This feature is illustrated in Fig. 5, which shows the curves of the dependence of the concentration of lead at points located on the axis of the fixed bed at different distances from its origin. Below, using an example of other adsorbate–adsorbent systems, another profile behavior will be demonstrated.

Dynamic Adsorption of Nitrates on PAN-oxime-nano

The authors of [17] investigated the dynamic process of water purification from nitrates on Fe_2O_3-coated PAN-oxime nanofiber as a sorbent. The sorbent PAN-oxime-nano was prepared by electrospinning of polyacrylonitrile nanofibers, which were then chemically modified with amidoxime groups. The effects of the flow rate of water passing through the sorption bed and of the sorption bed height L on the breakthrough curves was studied.

The circles in Fig. 6 show a breakthrough curve from [17] obtained by measuring the concentration of

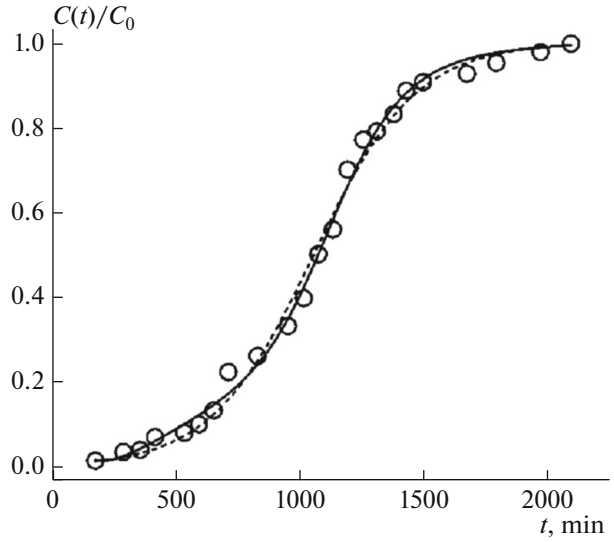

Fig. 6. Time dependence of the concentration ratio $C(t)/C_0$ for ions in the aqueous solution at the sorption column outlet. The circles are the experimental values from [17]. The solid line is the result of fitting theoretical dependence (9) to the experimental curve, whereas the dashed line is the result of fitting logistic function (4) with $a = 1$, $b(t) = b_0$, and $k(t) = k_0$ to experimental data.

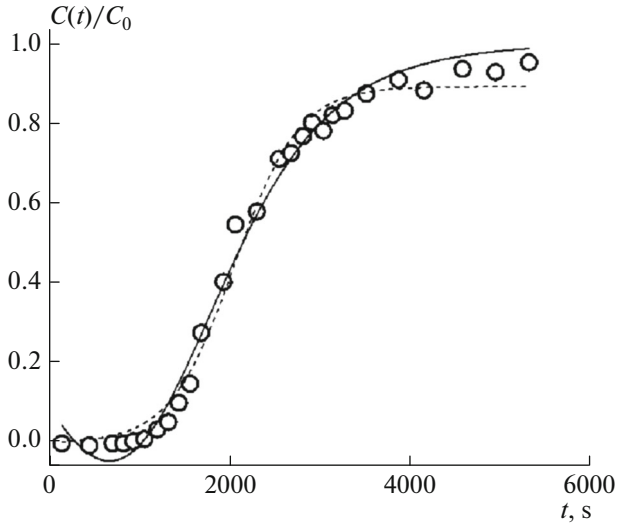

Fig. 7. Time dependence of the concentration ratio $C(t)/C_0$ for citric acid in the aqueous solution at the sorption column outlet. The circles are the experimental data from [19]. The solid line is the result of fitting theoretical dependence (9) to the experimental one, whereas the dashed line is the result of fitting logistic function (4), with $a = 1$, $b(t) = b_0$, and $k(t) = k_0$ to experimental data.

ions in the aqueous solution at the outlet of the sorption column at an effluent flow rate of 2.5 cm^3/min and an initial concentration of $C_0 = 0.05$ mg/cm^3. The geometric parameters of the fixed sorbent bed were $L = 150$ mm and $S = 0.2$ cm^2.

As in the case of the breakthrough curve for lead adsorption (Fig. 3), the experimental dependence shown in Fig. 6 was approximated by theoretical function (9). In addition, it was also approximated by logistic function (4) with $a = 1$, $b(t) = b_0$, and $k(t) = k_0$. The determination coefficient for the process of approximation of the experimental data by function (9) turned out to be $R^2 = 0.996399$, which is indicative of a very good fit, although it is somewhat lower than for fitting the breakthrough curve for the lead sorption. The values of the variable parameters obtained from the approximation are given in the table. It turned out that, like for lead, the coefficients b_3, b_4, k_2 of the higher terms of the power series expansion of the functions $b(t)$ and $k(t)$ represented by expression (7) are zeros.

As can be seen from Fig. 6, the difference between approximating functions (4) and (9) is insignificant. This is due to the fact that the form of the experimental curve differs little from that of the logistic function. To verify this, we used measured breakthrough curves for the dynamic process of water purification from citric acid on Amberlite IRA-67 anionite [19] (Fig. 7). The form of the experimental dependence differs significantly from that the logistic function, namely, it does not have the symmetry of the C_2 group with respect to the inflection point; i.e., the curve, when rotated by 180° relative to the axis perpendicular to the plane of the graph passing through the inflection point, does not coincide with itself. This figure also shows plots of functions (4) and (9), by which the experimental curve was fitted. It can be seen that the quality of fitting the theoretical dependences to the experimental data is low in both cases, but the shape of one theoretical curve (solid line), in contrast to the second curve (dashed line), does not have C_2 symmetry. This fact indicates that our approach is suitable for describing the breakthrough curves of much more complex forms than the logistic one.

Using the parameters presented in the table, the space–time concentration profile of NO_3^- ions in the fixed PAN-oxime-nano bed was calculated. A 3D profile in three project views is displayed in Fig. 8. In contrast to the concentration profile of lead in Fig. 4, this profile shows the following peculiarity: the time dependence of the nitrate concentration within the $0 < x < 100$-mm layer of the sorption bed is nonmonotonic. At large x, the dependence becomes monotonic. In order to verify this, we constructed, by analogy with Fig. 5, the dependence of the $C(t)/C_0$ ratio for nitrates in the fixed PAN-oxime-nano bed at points on the axis of the bed at different distances from its inlet (Fig. 9).

Figure 9 shows that curves *1–4* are nonmonotonic, whereas curves *5–7* are monotonic. The fact of the nonmonotonicity of the curves confirms the conclusion we drawn in one of the previous articles [16] that,

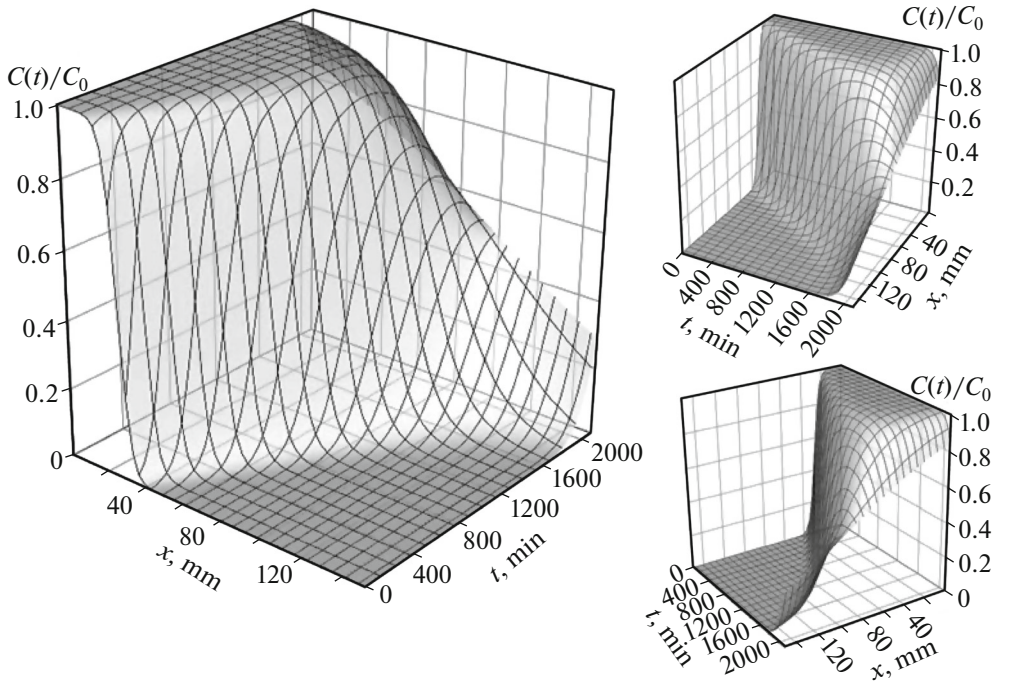

Fig. 8. Space–time concentration profile of NO_3^- in the fixed PAN-oxime-nano bed for water purification from nitrates.

during the adsorption process, the redistribution of adsorbate concentration in the fixed sorbent bed can be observed. For example, in layers of sorbent located 40 mm from the column inlet (curve *2*), the concentration of nitrates increases to the maximum value (C_0) within the first 800 min of the process, remains at this level for the next 1600 min, and then decreases. This behavior of nitrates in a fixed bed differs from that of lead (Fig. 5).

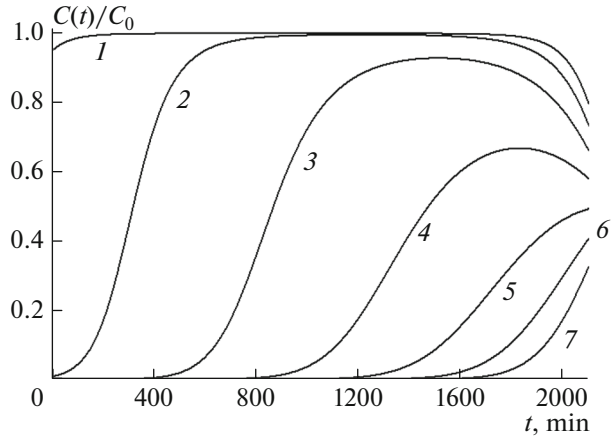

Fig. 9. Time dependence of the concentration ratio $C(t)/C_0$ for nitrates in the fixed PAN-oxime-nano bed at various points x (mm): (*1*) 20, (*2*) 40, (*3*) 60, (*4*) 80, (*5*) 100, (*6*) 120, and (*7*) 140.

Dynamic Adsorption of Perchlorates on CLDH

The paper [18] describes the study of the dynamic process of water purification from perchlorate ions using CLDH as a sorbent. In [18], CLDH sorbent was prepared by calcining layered double Al/Zn hydroxide in a muffle furnace at 500°C. Layered DH containing carbonate as an interlayer anion was synthesized by the traditional coprecipitation method. The influence of the water flow rate through the sorption bed on the breakthrough curves was studied.

Figure 10 shows an experimental breakthrough curve [18] relating to measuring the concentration of ClO_4^- ions in the aqueous effluent at the outlet of a sorption column, moving at a rate of 2 cm^3/min, for an initial concentration of $C_0 = 0.1$ mg/cm^3. The constants describing the geometry of the fixed sorbent bed are $L = 85$ mm, $S = 0.5$ cm^2. As in the cases of breakthrough curves for the adsorption of lead (Fig. 3) and nitrates (Fig. 6), that shown in Fig. 10 was approximated by theoretical dependence (9). The determination coefficient for fitting the experimental data by function (9) turned out to be $R^2 = 0.998401$, which indicates a high quality of fit, although it is somewhat lower that for the lead sorption, but higher than that for the sorption of nitrates.

The values of the variable parameters obtained from the fit are listed in the table. It turned out that, like for lead and nitrates, the coefficients b_3, b_4, k_2 of the higher terms in power series expansion (7) of the functions $b(t)$ and $k(t)$ are zeros.

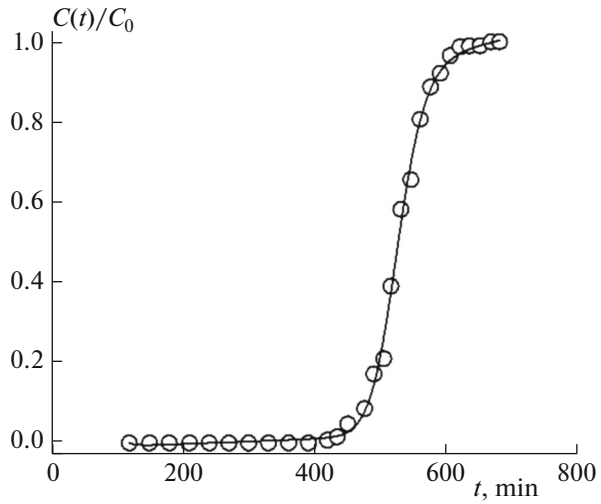

Fig. 10. Time dependence of the concentration ratio $C(t)/C_0$ for ClO_4^- ions in the aqueous solution at the sorption column outlet. The circles represent the experimental data from [18]. The curve is the result of fitting theoretical dependence (9) to the experimental one.

Using the values of the parameters presented in the table, the space–time concentration profile of ions in the fixed CLDH bed was calculated. A 3D profile in three project views is displayed in Fig. 11.

Similar to the concentration profile of nitrates (Fig. 8), but unlike the concentration profile of lead (Fig. 4), this profile exhibits a nonmonotonic time dependence of the concentration of perchlorates in the $0 < x < \sim 40$ layer of the sorption bed. This is most clearly seen from the time dependence of the concentration ratio $C(t)/C_0$ for perchlorates in a CLDH fixed bed at points on the axis of the bed at different distances from its inlet (Fig. 12).

The nonmonotonic time dependences of the concentrations of nitrates and perchlorates seen in Figs. 9 and 12 at some points of the fixed bed suggest that, in the course of the sorption process, the adsorbate concentration is redistributed: in layers near the sorption column inlet, it first increases, sometimes to the maximum possible values, and then begins to fall. In the next subsection, it is demonstrated that the total amount of adsorbate in the fixed bed increases monotonically throughout the entire sorption process.

Time Dependence of the Total Amount of Adsorbate in the Fixed Bed

The observed nonmonotonic behavior of the time dependence of the adsorbate concentration at certain points of the fixed bed, i.e., its redistribution inside the sorbent suggests that it is necessary to examine how the total amount of adsorbate $W(t)$ in the fixed bed changes with time. Obviously, this dependence can be calculated by multiplying definite integral (5) by the cross sectional area S of the bed:

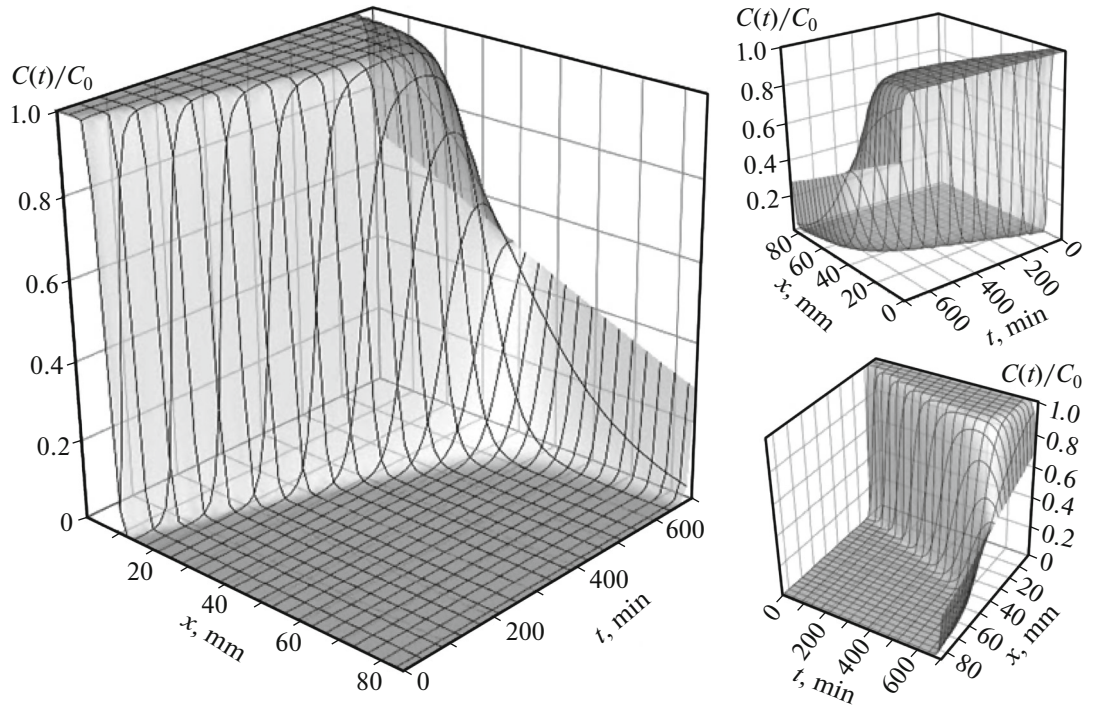

Fig. 11. Space–time concentration profile of ClO_4^- in the fixed CLDH bed for the purification of water from perchlorates.

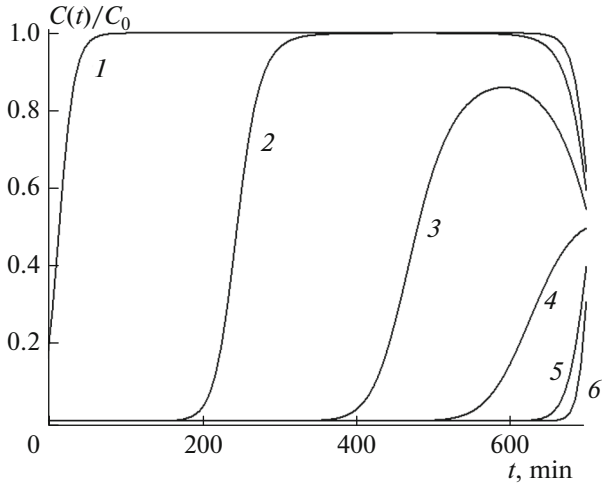

Fig. 12. Time dependence of the concentration ratio of $C(t)/C_0$ for perchlorate ions in the fixed CLDH bed at various points x (mm): (*1*) 10, (*2*) 20, (*3*) 30, (*4*) 40, (*5*) 60, and (*6*) 80.

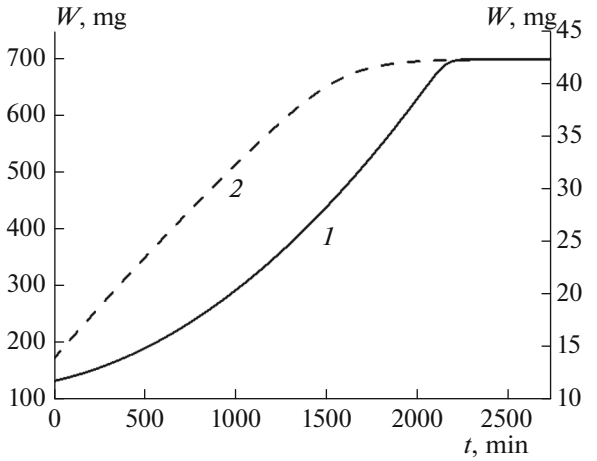

Fig. 13. Time dependence of the total amount of adsorbate in the fixed sorbent bed for (*1*) lead (right scale) and (*2*) nitrates (left scale).

$$W(t) = S\int_0^L q(x,t)dx = \frac{aS}{k(t)}\left\{\ln\frac{1+\exp\{k(t)[L-b(t)]\}}{1+\exp\{-k(t)b(t)\}}\right\}, \quad (11)$$

where $b(t)$ and $k(t)$ are determined by expressions (7), whereas the parameters b_0, b_1, b_2, b_3, b_4, k_0, k_1, and k_2 in these expressions, determined from the fitting procedure, are summarized in the table. The calculated dependences of $W(t)$ for the adsorption of lead and nitrates are displayed in Fig. 13.

Figure 13 shows that the total amount of adsorbate in the fixed sorbent bed increases monotonically for ~2000 min until it reaches a limiting value. For nitrates, this time of saturation of the sorbent with adsorbate approximately corresponds to the time it takes for the breakthrough curve of NO_3^- in Fig. 6 to level off onto a plateau. For the lead sorption, these times differ slightly: 1500 and 2000 min in Figs. 3 and 13, respectively, which is probably due to an incorrect estimate of the geometric parameters of the fixed bed in [14].

CONCLUSIONS

Thus, that the method for calculating the space–time concentration profiles of adsorbates $q(x, t)$ described in the article on the basis of experimental breakthrough curves $C(t)$ turned out to be very fruitful.

First, based on the logistic function dependence of the adsorbate concentration on the longitudinal axial coordinate of the fixed bed, it was possible to reproduce a rather complicated shape of the space–time concentration profile in the sorption column.

Secondly, it was possible to prove the existence of adsorbate redistribution in the sorbent bed during the sorption process.

Thirdly, it was shown that, despite local decreases in the adsorbate concentration in some layers, its total amount in the fixed sorbent bed increases monotonically with time throughout the adsorption process, reaching a saturation level.

For nitrates, the times of onset of saturation on the curve of the time dependence of the total amount of adsorbate in the fixed bed and on the breakthrough concentration curve at the column outlet are identical, whereas for lead, they are similar. Note also that the analytical formulas derived proved to be very convenient for calculations.

REFERENCES

1. W. J. Thomas and B. Crittenden, *Adsorption Technology and Design* (Butterworth-Heinemann, Elsevier, Oxford, 1998), pp. 104, 145.
2. M. A. Sohsah, M. M. Ghoneim, S. H. Othman, and B. E. El-Anadouli, in *Proceedings of the 8th Radiation Physics and Protection Conference, Beni Sueif-Fayoum, Egypt,* 2006, p. 415. http://www.iaea.org/inis/collection/NCLCollectionStore/_Public/38/092/38092990.pdf.
3. T. Hang and R. A. Dimenna, Contract 2003, Report No. DE-AC09-96SR18500, WSRC-MS-99-00943 (U.S. Department of Energy, 2003).
4. D. O. Cooney, Chem. Eng. Comm. 91, 1 (1990).
5. M. A. S. D. Barros, P. A. Arroyo, and E. A. Silva, *Mass Transfer-Advances in Sustainable Energy and Environment Oriented Numerical Modeling,* Ed. by H. Nakajima (InTech, Croatia, 2013). doi 10.5772/51954
6. V. K. Gupta, Ind. Eng. Chem. Res. 37, 192 (1998).
7. I. V. Kumpanenko, A. V. Roshchin, N. A. Ivanova, A. V. Bloshenko, et al., Russ. J. Phys. Chem. B 11 (2017, in press).

8. D. Tondeur, A. Gorius, and M. Bailly, in *Adsorption: Science and Technology,* Ed. by A. E. Rodrigues et al., Vol. 158 of *NATO Adv. Sci. Inst., Ser. E* (Kluwer, Dordrecht, 1989), p. 115.
9. C. Tien, *Adsorption Calculations and Modeling,* Ed. by H. Brenner (Elsevier, Netherlands, 1994).
10. S. Afzal, A. Rahimi, M. R. Ehsani, and H. Tavakoli, J. Ind. Eng. Chem. 16, 978 (2010).
11. A. M. Egorin and V. A. Avramenko, Radiochemistry 54, 483 (2012).
12. M. Gholami, M. R. Talaie, and S. F. Aghamiri, Gas Process. J. 1 (2), 22 (2013).
13. N. Ping, G. Junjie, and H.-J. Bart, Chin. J. Chem. Eng. 5, 304 (1997).
14. J. T. Nwabanne and P. K. Igbokwe, J. Pure Appl. Sci. 6, 2009 (2012).
15. I. V. Kumpanenko, A. V. Roshchin, N. A. Ivanova, V. V. Novikov, A. M. Skryl'nikov, A. M. Podvalny, and V. V. Usin, Russ. J. Phys. Chem. B 11, 154 (2017).
16. I. V. Kumpanenko, A. V. Roshchin, N. A. Ivanova, A. V. Bloshenko, et al., Russ. J. Phys. Chem. B 11 (4), 568 (2017).
17. M. Jahangiri-rad, A. Jamshidi, M. Rafiee, and R. Nabizadeh, J. Environ. Health Sci. Eng., 1 (2014). http://www.ijehse.com/content/12/1/90.
18. X. Wu, Y. Wang, L. Xu, and L. Lv, Desalination 256, 136 (2010).
19. P. Gluszcz, T. Jamroz, B. Sencio, and S. Ledakowicz, Bioprocess. Biosyst. Eng. 26, 185 (2004).

Translated by V. Smirnov